A MEMS-Based Wide-Band Multi-State Power Attenuator for Radio Frequency and Microwave Applications

J. Iannacci[*], A. Faes[*], F. Mastri[**], D. Masotti[***] and V. Rizzoli[***]
[*]Fondazione Bruno Kessler – FBK, MEMS Research Group,
Via Sommarive 18, 38123, Povo - Trento, ITALY, iannacci@fbk.eu
[**]University of Bologna, DIE Department, Bologna, ITALY
[***]University of Bologna, DEIS Department, Bologna, ITALY

ABSTRACT

In this work we present a novel implementation of a multi-state RF (Radio Frequency) power attenuator, entirely realized in MEMS (MicroElectroMechanical-Systems) technology. The network, based on a CPW (Coplanar Waveguide) structure and fabricated in FBK technology, features several resistors realized with an highly-doped poly-silicon layer. Each resistor can load the RF line or can be shorted, depending on the state (actuated/not-actuated) of electrostatically controlled suspended-membrane-based MEMS switches. The network realizes 128 attenuation levels with flat characteristics over broad frequency ranges.

The network features two sections, namely a series and a parallel one, that are experimentally characterized in a few of the possible configurations up to 30 GHz and simulated within CST™ Microwave Studio.

After validating the simulated results for the two sections, simulated results of the whole RF-MEMS-based power attenuator are presented and discussed.

Keywords: RF-MEMS, power attenuator, reconfigurability, electromagnetic simulations

1 INTRODUCTION

MEMS (MicroElectroMechanical Systems) technology for Radio Frequency applications (i.e. RF-MEMS) has emerged in recent years as a valuable solution to manufacture low-cost and high-performance passive components, like variable capacitors, inductors and micro-switches [1,2]. Together with the demonstration of RF-MEMS lumped components, the interest and the efforts of research have been focusing on their exploitation as basic elements, in order to fabricate complex functional blocks and networks able to handle and process RF and Microwave signals. Some valuable examples of entirely RF-MEMS-based networks are available in literature, concerning phase shifters [3,4] and TTD-lines (True Time Delay) [5] for antenna and radar applications, reconfigurable impedance matching networks [6] and switching matrices for the channels selection in satellites and terrestrial communication platforms [7]. All of the listed examples exhibit good performances and high reconfigurability, extending the functionalities of the whole architecture employing an RF-MEMS block.

Specifically, this work will focus on another emerging class of RF-MEMS complex networks, represented by reconfigurable power attenuators, being them suitable for various applications. For instance, RF power attenuators are commonly used in order to match the VSWR (Voltage Standing Wave Ratio) to the desired value in order to improve the input match of a Power Amplifier (PA) at a certain frequency. It is straightforward that, in a scenario calling for an increasing reconfigurability of RF platforms, the availability of power attenuators able to fully address such a requirement is positively saluted by the Scientific Community. Up to now, implementations of RF power attenuators are not easy to find in literature as for the other MEMS-based networks mentioned above (e.g. phase shifters and so on). Consequently, one should rely on standard implementations of power attenuators, that, however, exhibit narrow frequency range and limited reconfigurability [8]. Furthermore, such networks are typically rather bulky, as they are not manufactured within a microelectronics technology platform, but rather are based on discrete components mounted on a PCB (Printed Circuit Board).

Given the just discussed motivations, we designed, fabricated and tested the MEMS-based multi-state RF power attenuator that is discussed in this paper. Being the network conceived as a general purpose demonstrator, we did not have in mind a specific frequency range for its operation. Consequently, we designed it aiming at having a large frequency range, with a significant number of attenuation levels (i.e. large reconfigurability), and with a good flatness of each level over the whole frequency span.

The network we propose realizes different attenuation levels by means of banks featuring high-resistivity poly-silicon resistors connected in series. Each resistor can load the RF lines or be shorted, depending on the state of electrostatically actuated suspended gold membranes.

The paper is arranged as follows: *Section 2* reports details concerning the employed technology platform. *Section 3* shows the topology of the proposed network and a few electromechanical measurements. *Section 4* discusses the RF measured and simulated performances of the reconfigurable power attenuator. At last, *Section 5* collects a few final consideration about the work.

2 FBK RF-MEMS TECHNOLOGY PLATFORM

The reconfigurable power attenuator discussed in this paper is fabricated in the RF-MEMS surface micromachining process available at FBK in Italy. As an example of this technology process features, a schematic of an ohmic series cantilever relay is reported in Fig. 1.

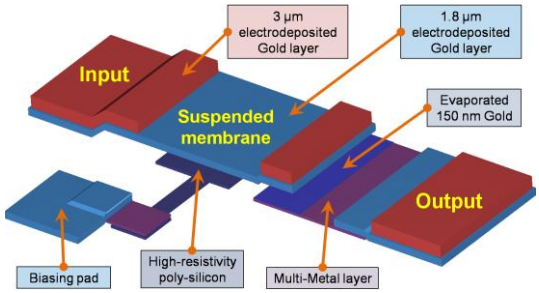

Figure 1: Schematic 3D view of a cantilever-based ohmic relay in FBK RF-MEMS technology.

A double-dose Boron implanted poly-silicon layer enables areas with very high-resistance (~1.5 kΩ/sq), suitable for DC biasing electrodes and lines, and parts with medium resistance (30-300 Ω/sq), useful for RF and DC resistive loads. The second conductive layer is a sandwiched multi-layer based on Aluminum, and is mainly exploited for RF signals [9]. The electrodeposited layer of Gold with different thickness (1.8 µm and 3.0 µm) defines the CPWs (Coplanar WaveGuides) and microstrips, as well as the suspended MEMS membranes, where a sacrificial photoresist is deposited before the Gold deposition. In addition, a 150 nm Gold layer is evaporated on the ohmic contact areas beneath the suspended MEMS structures, in order to establish a Gold-to-Gold contact when the switches are electrostatically actuated.

3 RF-MEMS RECONFIGURABLE POWER ATTENUATOR

The proposed RF power attenuator is based on highly-doped poly-silicon resistors connected in series. Each resistor loads the in/out RF line or is shorted, depending on the state (not actuated or actuated, respectively) of electrostatically operated MEMS gold membranes. A microphotograph of the entire network is reported in Fig. 2-left. The network comprises two sections, namely, the *series section*, with 3 resistors in series (labels "1" to "3" in Fig. 2-right), and a *parallel section*, with two branches (with 3 resistors each) in parallel (labels "5" to "7"). The latter one features also two additional MEMS membranes (i.e. series-ohmic switches) singularly operable, in order to select one or both the resistive branches (labeled as "4-A" and "4-B"). The network of Fig. 2 realizes $2^{3+1+3} = 128$ different attenuation states.

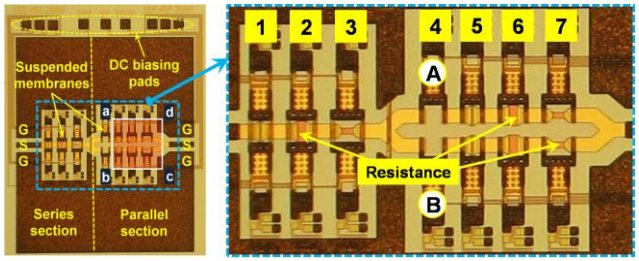

Figure 2: *Left*. Microphotograph of the RF power attenuator. The dashed part in the parallel section is reported in Fig. 3. *Right*. Close-up of the 7 MEMS switches ("1" to "3": series section; "4" to "7" parallel section).

Fig. 3 shows the 3D profile, measured with an optical profilometer based on interferometry, of the 3 resistive loads (R_1, R_2, R_3) of the parallel section (i.e. the region highlighted in the "abcd" square in Fig. 2-left).

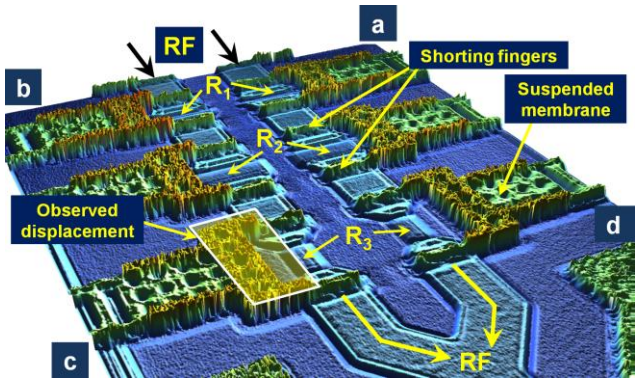

Figure 3: 3D profile of the parallel section (see Fig. 2). The "abcd" corners correspond to the ones of Fig. 2-left. The vertical displacement vs. applied bias of the highlighted membrane (in the bottom-left) is shown in the next Fig. 4.

The static pull-in/pull-out characteristic of the suspended membranes is characterized with the optical profilometer by using a stroboscopic light [10]. The applied bias is a triangular zero mean value symmetric voltage, swept between -40 V and +40 V. The vertical displacement vs. bias is reported in Fig. 4.

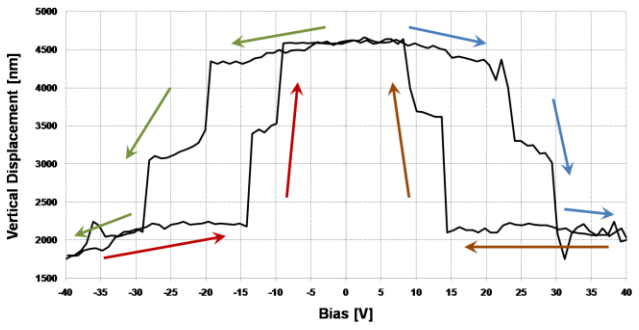

Figure 4: Measured pull-in/pull-out characteristic of the MEMS membrane highlighted in Fig. 3.

A two-steps pull-in and pull-out is visible between ±20-30 V and ±8-15 V, respectively. This behavior is due to the topology of the suspended MEMS structures. Indeed, being the membrane hinged only on one side (i.e. cantilever-like) the free end is the first one to pull-in. Subsequently, as the bias further increases, also the remaining part of the structure collapses onto the underlying electrode, causing the second pull-in/pull-out.

4 RF CHARACTERISTICS

A few RF attenuator fabricated samples have been experimentally characterized. The poly-silicon layer adopted for the resistive loads has a sheet-resistance of 250 Ω/sq on the quartz wafer containing the DUTs (Devices Under Test). Consequently, according to the form factor of the resistors highlighted in Fig. 2, their value is 25 Ω for sections "1, 5", 100 Ω for sections "2, 6" and 250 Ω for sections "3, 7". Within the fabrication batch, various Boron doses have been implanted in order to obtain resistors with different values.

The series and parallel sections (see Fig. 2) are available also as standalone samples, and they have been separately characterized as the samples comprising both sections were not yet available when the measurements were performed.

A series section sample is measured (S-parameters from 100 MHz to 13.5 GHz) when the 3 resistances are loading the RF line (i.e. sections "1" to "3" not actuated), and when section "3" is actuated. Moreover, the network has been simulated within CST™ Microwave Studio in the same conditions. Fig. 5 shows the behavior of the simulated and measured curves (S21 parameter).

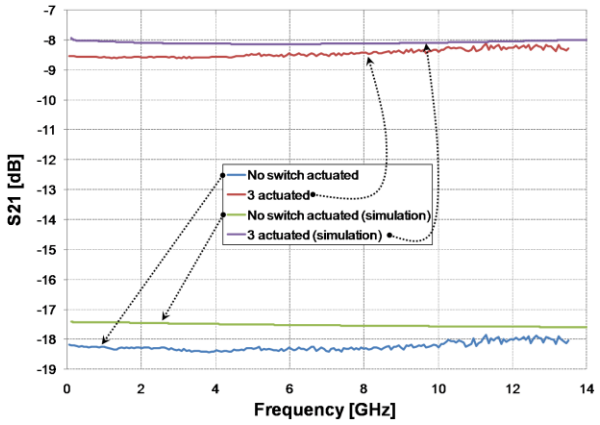

Figure 5: S21 parameter characteristic (measured and simulated from 100 MHz to 13.5 GHz) of the series section, when none and when section "3" is actuated (see Fig. 2).

The measured characteristic of the S21 parameter is rather flat over the whole frequency span in both cases (variation of less than 0.5 dB), and shorting the 250 Ω load reduces the attenuation of about 9.5 dB. The simulated curves well compare with the measurements. The simulated attenuation levels are lower than the measurements of about 0.5 dB. However, being the poly-silicon resistivity of 250 Ω/sq an average on-wafer value admitting a variation range of ±37 Ω/sq, very likely the actual poly-silicon resistivity of the measured sample is larger.

A parallel section sample has been also characterized with a different VNA (Vector Network Analyzer), enabling measurement from 100 MHz up to 30 GHz. A few attenuation levels, comprised between the min and max ones, are reported in Fig. 6. Moreover, the latter two levels have also been simulated.

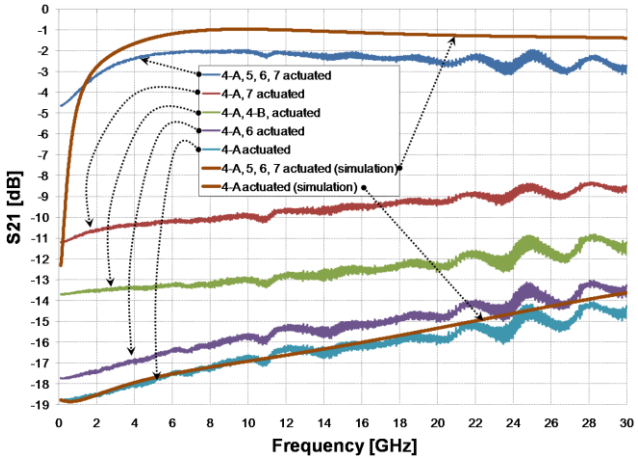

Figure 6: S21 parameter characteristic (measured from 100 MHz to 30 GHz) of the parallel section, corresponding to a few possible states of the RF network. Simulated curves for the min and max levels are also reported.

The min attenuation is obtained when the 3 resistive loads are shorted ("4-A, 5, 6, 7 actuated" in Fig. 6), while the max value is reached when the 3 resistors load the RF line and only one branch is selected ("4-A actuated"). The S21 characteristics are rather flat, since the variation over the large analyzed frequency span is smaller than 3 dB, while the attenuation range is broad (e.g. 15 dB at 10 GHz). The difference between the selection of one or both branches (loads in parallel) is visible comparing the "4-A actuated" and "4-A, 4-B actuated" curves, respectively, leading to a difference of 4-5 dB over the whole range.

The simulated curves (min and max levels) well compare with the measurements. Concerning the min level, the S21simulated curve presents a difference with respect to the measurement of about 1 dB above 4 GHz. This can be explained with the metal-to-metal contact resistance of the actuated membranes in the physical device, not accounted for in the simulation, where such a contact is ideal. The large difference up to about 1 GHz is most probably due to numerical issues of the FEM simulator at low frequency.

All the MEMS membranes have been actuated with DC bias levels ranging between 70 V and 80 V.

After the validation of the results simulated with CST against experimental results, the FEM tool was exploited to simulate the behavior of the whole RF power attenuator

reported in Fig. 2. The S21 parameter characteristics up to 40 GHz are reported in Fig. 7 for a few network configurations, between the min and max attenuation levels.

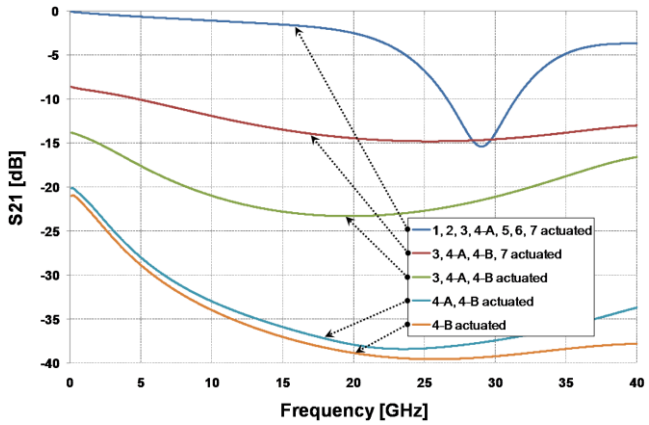

Figure 7: S21 parameter characteristic of the entire RF-MEMS network simulated within CST in a few different configurations. The labels refer to the attenuator stages described in Fig. 2.

A difference of about 36 dB between the min and max attenuation levels is reached at 20 GHz. Moreover, the difference due to the selection of one or both the resistive branches in the parallel section is visible in the lower portion of the plot.

Finally, the qualitative behavior of the loss density has been preliminarily investigated in CST (see Fig. 8). The right port of a parallel section was excited with a 30 dBm RF signal at 10 GHz. In this simulation all the conductive layers have been considered as PECs (Perfect Electric Conductors). It is significant the larger loss density of the membranes on the left (sections "4-A" and "4-B" in Fig. 2) compared to sections "5" to "7", as they are the only ones actuated (i.e. the RF signal flows through them).

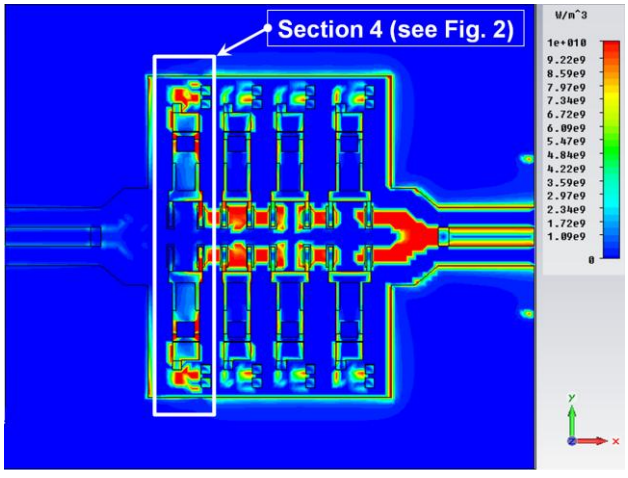

Figure 8: Simulated map of the loss density (W/m^3) in a parallel section. The right port is excited with a 30 dBm RF power at 10 GHz. Sections "4-A" and "4-B" are actuated.

5 CONCLUSIONS

In this work we presented a MEMS-based multi-state power attenuator for RF and Microwave signals. The network features several resistors, realized in highly-doped poly-silicon, and each of them can load the RF line or be shorted, depending on the state of electrostatically controlled MEMS ohmic switches. The network features two sections (series and parallel) and each of them has been experimentally characterized (S-parameters) and simulated, showing large span of attenuation levels and good flatness up to 30 GHz. After the validation against measurements of the network subsections simulations, a few of the 128 attenuation levels enabled by the whole network have been simulated. In addition, a qualitative loss density map was shown, as the further issue that will be investigated in the near future is the power handling. To our knowledge, the presented work is one of the first attempts to implement a reconfigurable RF power attenuator in MEMS technology.

REFERENCES

[1] S. Hyung et Al., "High-Q, tunable-gap MEMS variable capacitor actuated with an electrically floating plate", in Proc. of the IEEE MEMS Int. Conf., pp. 180-183, Jan. 2008.

[2] Zine-El-Abidine et Al., "A new class of tunable RF MEMS inductors", in Proc. of MEMS, NANO and Smart Systems Int. Conf., pp. 114-115, Jul. 2003.

[3] K. Topalli et Al., "A Monolithic Phased Array using 3-bit DMTL RF MEMS Phase Shifters", IEEE T-MTT, Vol. 56, No. 2, pp. 270-277, Feb. 2008.

[4] B. Pillans et Al., "Ka-Band RF MEMS Phase Shifters", IEEE Microwave and Guided Wave Letters, Vol. 9, No. 12, pp. 520-522, Dec. 1999.

[5] H. J. De Los Santos, "RF Mems Circuit Design for Wireless Communications", Artech H., 2002.

[6] L. Larcher et Al., "A MEMS Reconfigurable Quad-Band Class-E Power Amplifier for GSM Standard", in Proc. of the IEEE MEMS Int. Conf., pp. 864-867, Jan. 2009.

[7] M. Daneshmand et Al., "Redundancy RF MEMS Multi-Port Switches and Switch Matrices", IEEE/ASME Journal of MEMS, Vol. 16, No. 2, pp. 296-303, Apr. 2007.

[8] T. Kantasuwan, R. Ramzan and J. Dąbrowski, "Programmable RF Attenuator for On-Chip Loopback Test", in Proc. of the 10th IEEE European Test Symposium ETS, May 2005.

[9] K. Rangra, "Symmetric toggle switch—a new type of rf MEMS switch for telecommunication applications: Design and fabrication", Elsevier Sens. and Act. A: Physical, Vol. 123-124, 2005, pp. 505-514.

[10] E. Novak, D.-S. Wan, P. Unruh, M. Schurig, "MEMS Metrology Using a Strobed Interferometric System", in Proc. of the IMEKO Con., pp. 178-182, Nov. 2003.